

## **Toward a Global 1/25° HYCOM Ocean Prediction System with Tides**

Eric P. Chassignet

Center for Ocean-Atmospheric Prediction Studies, Florida State University  
phone: (850) 644-4581 fax: (850) 644-4841 email: [echassignet@coaps.fsu.edu](mailto:echassignet@coaps.fsu.edu)

Award #: N00014-09-1-0587

<http://www.hycom.org>

### **LONG-TERM GOALS**

The overall technical goal is to implement a 1/25° horizontal resolution global ocean prediction system based on the HYbrid Coordinate Ocean Model (HYCOM) with tides and dynamic sea ice. The scientific goals include but are not limited to a) evaluation of the internal tides representation in support of field programs, b) data assimilation in the presence of tides, c) evaluation of the model's ability to provide useful boundary conditions to high resolution coastal models, d) interaction of the open ocean with ice, e) shelf–deep ocean interactions, f) upper ocean physics including mixed layer/sonic depth representation, g) mixing, etc.

### **OBJECTIVES**

Work closely with NRL Stennis and NOPP HYCOM partners to (1) perform the R&D necessary to develop, evaluate, and investigate the dynamics of 1/25° global HYCOM with tides coupled to CICE (the Los Alamos sea ice model) with atmospheric forcing only, with data assimilation via NCODA (NRL Coupled Ocean Data Assimilation), and in forecast mode and (2) to incorporate advances in dynamics and physics from the science community into the HYCOM code.

### **APPROACH**

A series of HYCOM configurations is used to (a) evaluate internal tides representation, (b) implement a configuration for data assimilation in the presence of tides, and (c) investigate the interaction of the open ocean with ice. HYCOM development is the result of collaborative efforts among the Florida State University, University of Miami, and the Naval Research Laboratory (NRL) as part of the multi-institutional HYCOM Consortium for Data-Assimilative Ocean Modeling (Bleck, 2002; Chassignet et al., 2003; Halliwell, 2004). This effort was funded by the National Ocean Partnership Program (NOPP) to develop and evaluate a data-assimilative hybrid isopycnal-sigma-pressure (generalized) coordinate ocean model (Chassignet et al., 2009). HYCOM has been configured globally and on basin scales at up to 1/25° (~3.5 km mid-latitude) resolution. More details on the latest global simulations can be found at <http://www.hycom.org> and in the separate ONR report on NRL activities by A. Wallcraft.

<b>Report Documentation Page</b>			<i>Form Approved OMB No. 0704-0188</i>	
<p>Public reporting burden for the collection of information is estimated to average 1 hour per response, including the time for reviewing instructions, searching existing data sources, gathering and maintaining the data needed, and completing and reviewing the collection of information. Send comments regarding this burden estimate or any other aspect of this collection of information, including suggestions for reducing this burden, to Washington Headquarters Services, Directorate for Information Operations and Reports, 1215 Jefferson Davis Highway, Suite 1204, Arlington VA 22202-4302. Respondents should be aware that notwithstanding any other provision of law, no person shall be subject to a penalty for failing to comply with a collection of information if it does not display a currently valid OMB control number.</p>				
1. REPORT DATE <b>2009</b>	2. REPORT TYPE	3. DATES COVERED <b>00-00-2009 to 00-00-2009</b>		
4. TITLE AND SUBTITLE <b>Toward a Global 1/25degree HYCOM Ocean Prediction System with Tides</b>			5a. CONTRACT NUMBER	
			5b. GRANT NUMBER	
			5c. PROGRAM ELEMENT NUMBER	
6. AUTHOR(S)			5d. PROJECT NUMBER	
			5e. TASK NUMBER	
			5f. WORK UNIT NUMBER	
7. PERFORMING ORGANIZATION NAME(S) AND ADDRESS(ES) <b>Florida State University,Center for Ocean-Atmospheric Prediction Studies,Tallahassee,FL,32306</b>			8. PERFORMING ORGANIZATION REPORT NUMBER	
9. SPONSORING/MONITORING AGENCY NAME(S) AND ADDRESS(ES)			10. SPONSOR/MONITOR'S ACRONYM(S)	
			11. SPONSOR/MONITOR'S REPORT NUMBER(S)	
12. DISTRIBUTION/AVAILABILITY STATEMENT <b>Approved for public release; distribution unlimited</b>				
13. SUPPLEMENTARY NOTES				
14. ABSTRACT				
15. SUBJECT TERMS				
16. SECURITY CLASSIFICATION OF:			17. LIMITATION OF ABSTRACT <b>Same as Report (SAR)</b>	18. NUMBER OF PAGES <b>13</b>
a. REPORT <b>unclassified</b>	b. ABSTRACT <b>unclassified</b>	c. THIS PAGE <b>unclassified</b>	19a. NAME OF RESPONSIBLE PERSON	

## RESULTS

### Internal wave representation in Oceanic General Circulation Models (OGCMs)

In order to investigate the impact of the model grid spacing and vertical coordinate choice on the representation of internal waves in OGCMs and HYCOM in particular, we performed a multi-model study of internal wave generation, propagation, and evolution. The configuration is a stratified channel with a barotropic tide interacting with a Gaussian ridge (Khatiwala, 2000; Di Lorenzo et al., 2003; Legg and Huijst, 2006). The models that were evaluated are the HYbrid Coordinate Ocean Model (HYCOM, hybrid vertical coordinate), the Regional Ocean Modeling System (ROMS, terrain-following vertical coordinate), and the MITgcm (geopotential vertical coordinate). These models were chosen because of their different vertical coordinates and their wide usage by the community for global, regional, and coastal applications. Figure 1 shows the cross-vertical section of the zonal baroclinic velocity after 5 days for two of the models, HYCOM (run in isopycnal mode) and ROMS, for different horizontal grid spacing and for a particular critical wave regime (the steepness parameter, ratio of the topography slope to the internal wave beam angle, is close to 1). The model results are in reasonably good agreement with the theoretical results for high horizontal resolution, but the baroclinic response is considerably weaker in the coarse horizontal resolution simulations since they are unable to resolve the higher internal wave modes. In ROMS with the coarse horizontal resolution, the grid stiffness ratio parameter is violated and smoothing of the bathymetry is required. Such smoothing can lead to an underestimation of the tidal conversion process up to 50% (Di Lorenzo et al., 2003).

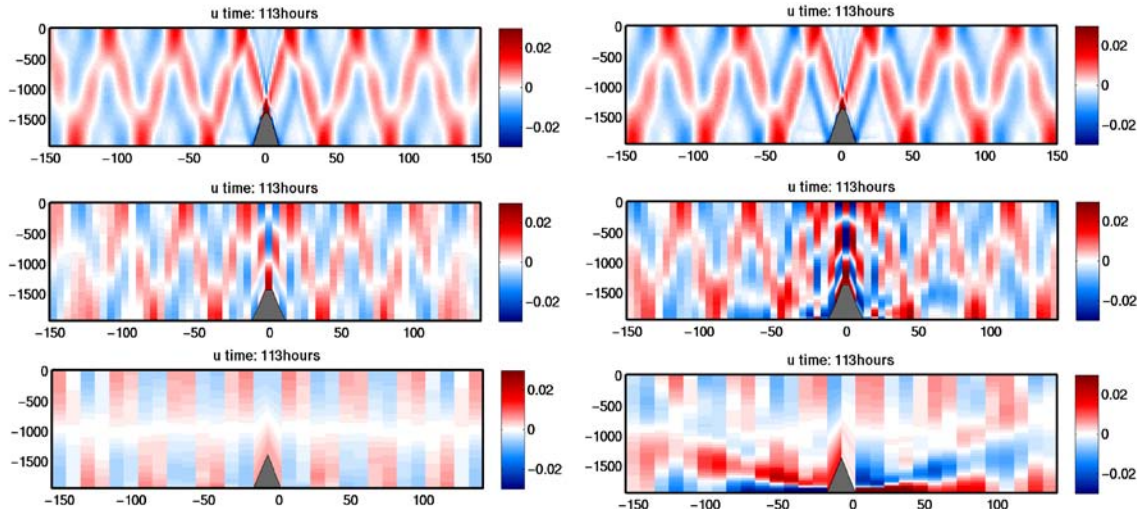


**Figure 1:** Snapshots (~4.7 days) of cross-vertical section of zonal baroclinic velocity for HYCOM (left panels) and ROMS (right panels). The horizontal model resolution is  $\Delta x = 1.5$  km for top panels,  $\Delta x = 5$  km for middle panels, and  $\Delta x = 10$  km for bottom panels. There are 100 layers/levels ( $\Delta z = 20$  m) in the vertical for both models.

### Diagnosing spurious mixing in fixed coordinate ocean models

Due to their numerical formulation, fixed vertical coordinate models are not able to preserve adiabatic properties of advected water parcels (Griffies et al., 2000). This numerically-induced diapycnal mixing can in some cases be of the same magnitude as naturally occurring mixing. There are only few studies that have attempted to document and quantify this spurious diapycnal mixing (Griffies et al., 2000;

Morales Maqueda, 2007; Holloway, 2007; Riemenscheider and Legg, 2007; Burchard and Rennau, 2008). In order to document and quantify the spurious mixing introduced by internal tides in both ROMS and the MITgcm, we used two idealized configurations: 1) the well known lock exchange problem (Haidvogel and Beckman, 1999) as a reference and 2) the pure internal wave field described in the previous section. For both experiments, no explicit mixing is prescribed and thus the initial water masses should remain at all times. We use the tracer flux method described by Griffies et al. (2000) to compute the spurious numerically-induced diapycnal diffusivity for both scenarios. Figure 2 and Figure 3 show snapshots of the temperature field at  $t = 20$  hr for the lock exchange problem for different resolution and advection schemes. The two densities initially present have diffused and have “leaked” into new density classes due to the numerically-induced mixing. Figure 4 and Figure 5 show Hovmöller plots of the diapycnal diffusivity using ROMS and the MITgcm (respectively) for the same experiments. The two figures show that finer model grid resolution decreases the numerical diffusion, but do not particularly improve the under/overshoots of temperature when high-order advection schemes (i.e. U3H and 3<sup>rd</sup> order upwind DST) are used. The periodicity of 2.5 hr in the diapycnal diffusivity signal is due to the natural seiche of the domain. These results compare very well with a recent study by Burchard and Rennau (2008).

Figure 6 shows the ROMS tidally averaged diapycnal diffusivity (tidal cycle 7) for the internal wave configuration using the MPDATA scheme. The higher magnitudes for diapycnal diffusivity are found for the densest density classes that correspond to steep slopes in the ROMS  $\sigma$ -levels. When the model resolution increases, the spurious diapycnal diffusivities magnitudes are reduced.

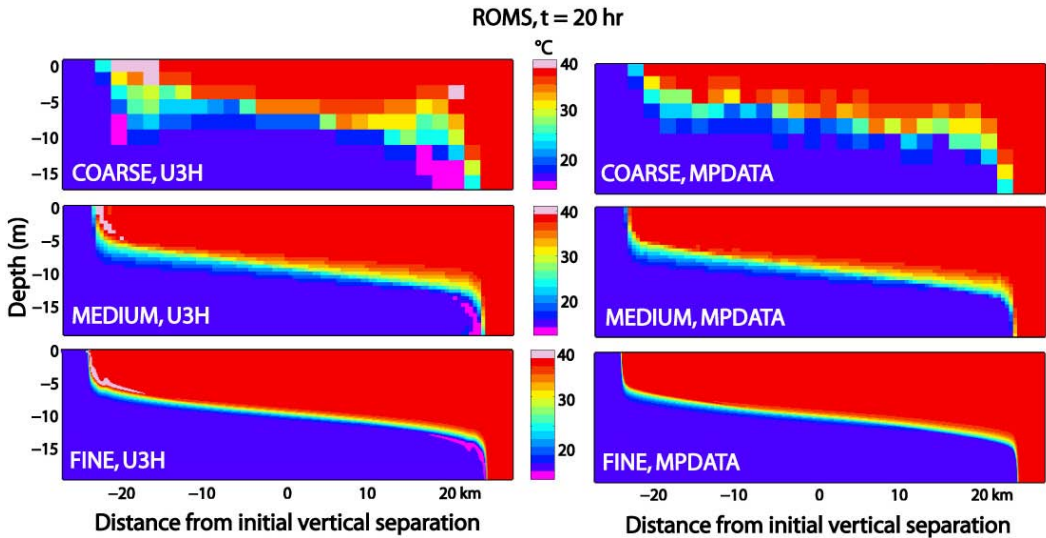


**Figure 2:** ROMS snapshots of the temperature field for the 3<sup>rd</sup> order upstream biased advection scheme (left panels, Schepetkin and Mc Williams, 2000) and the MPDATA scheme (right panels). The top panels are the COARSE experiments with  $\Delta x = 2000$  m and 10  $\sigma$ -levels, the middle panels are the MEDIUM experiment with  $\Delta x = 500$  m and 40  $\sigma$ -levels, the bottom panels are the FINE experiment with  $\Delta x = 125$  m and 160  $\sigma$ -levels.

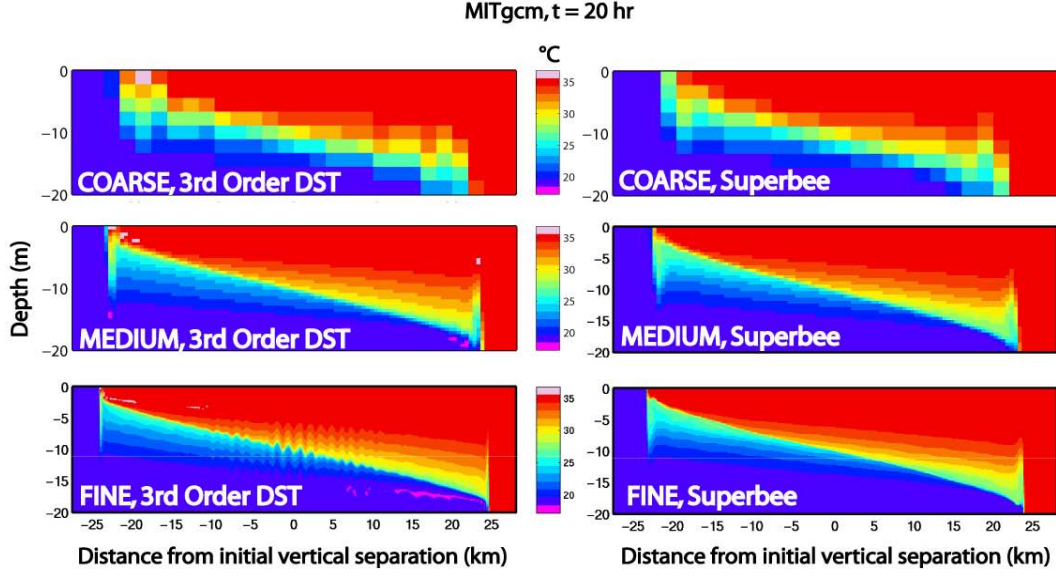


**Figure 3:** MITgcm snapshots of the temperature field for the 3<sup>rd</sup> order upwind DST advection scheme (left panels) and the Superbee scheme (right panels). The top panels are the COARSE experiments with  $\Delta x = 2000$  m and 10  $\sigma$ -levels, the middle panels are the MEDIUM experiment with  $\Delta x = 500$  m and 40  $\sigma$ -levels, the middle panels are the FINE experiment with  $\Delta x = 125$  m and 160  $\sigma$ -levels. The MITgcm need a higher viscosity parameter than ROMS to preserve model stability.

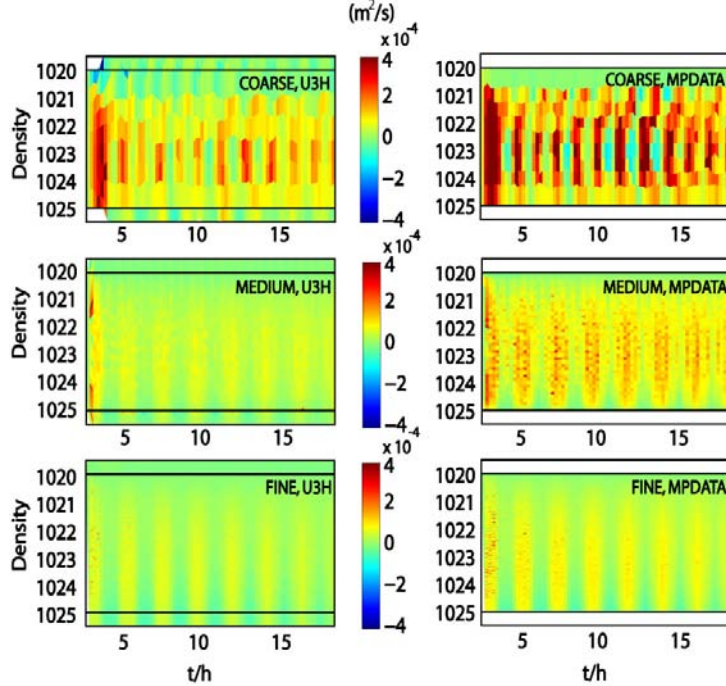


**Figure 4:** ROMS Hovmöller plots of the vertically averaged diapycnal diffusivity ( $\text{m}^2/\text{s}$ ). The top panels are the COARSE experiments with  $\Delta x = 2000$  m and 10 levels, the middle panels are the MEDIUM experiment with  $\Delta x = 500$  m and 40 levels, the middle panels are the FINE experiment with  $\Delta x = 125$  m and 160 levels.

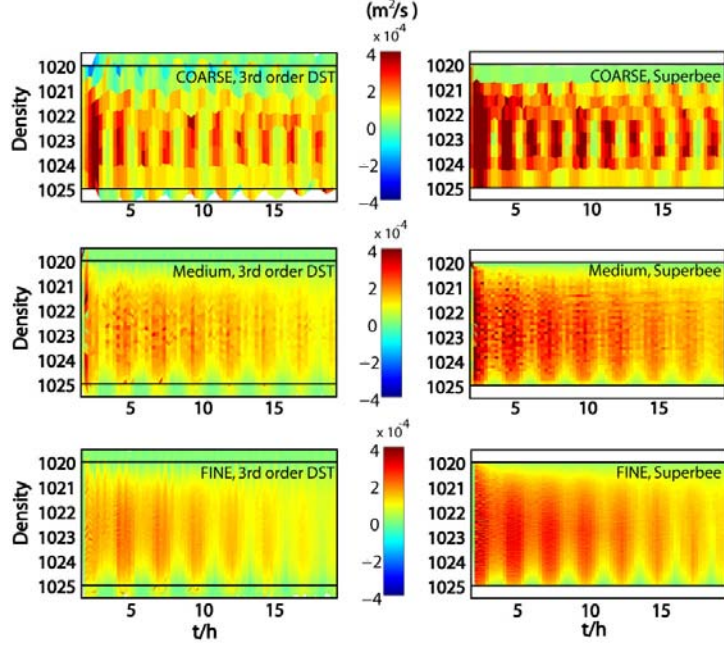


**Figure 5:** MITgcm Hovmöller plots of the vertically averaged diapycnal diffusivity ( $\text{m}^2/\text{s}$ ). The top panels are the COARSE experiments with  $\Delta x = 2000 \text{ m}$  and 10 levels, the middle panels are the MEDIUM experiment with  $\Delta x = 500 \text{ m}$  and 40 levels, the middle panels are the FINE experiment with  $\Delta x = 125 \text{ m}$  and 160 levels.

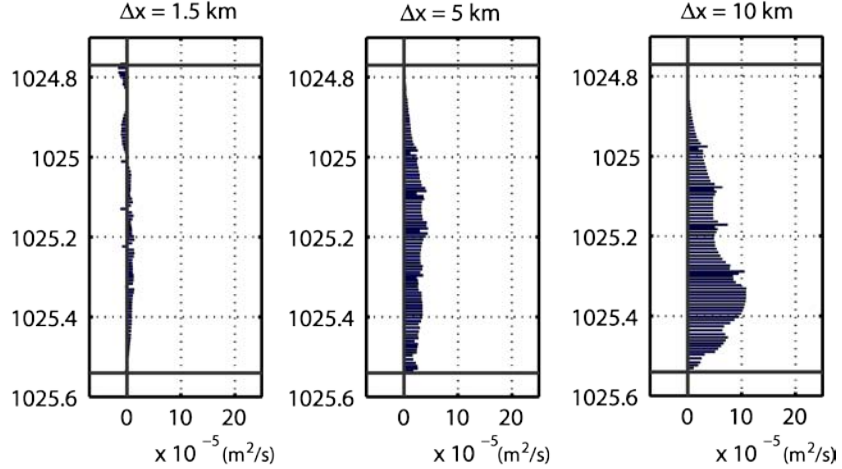


**Figure 6:** Tidally averaged (over tidal cycle 7) diapycnal diffusivity for the ROMS-MPDATA internal wave experiment with 100 levels. Left panel is using  $\Delta x = 1.5 \text{ km}$ , middle panel is using  $\Delta x = 5 \text{ km}$ , and right panel is using  $\Delta x = 10 \text{ km}$ .

## Data assimilation and tides

Assimilation systems typically consist of multiple interacting components for data handling, pre/post-processing module and analysis. The assimilation schemes available for HYCOM were all developed independently by the different assimilation groups and each of these schemes use different data formats, file naming conventions, metadata and interfaces between the different components. Early on, faced with the situation of handling multiple data formats and interfaces, we quickly realized that in order to be able to compare these schemes, we needed to standardize their data flow and data handling

infrastructure. This led to the development of a HYCOM “data assimilation toolbox” (Srinivasan et al., 2009). This “toolbox” is currently configured for the Gulf of Mexico (GOM) which is an ideal setting for exploring the performance of assimilation schemes because of its circulation features, limited size, data availability and interesting dynamics. The GOM forms a semi-enclosed sea connected to the Caribbean Sea by the Yucatan Channel in the South, and to the Atlantic Ocean in the East by the Florida Straits. It consists of a deep central basin surrounded by a broad shelf and its circulation is dominated by the Loop Current. The northern intrusion of the Loop Current into the GOM is highly variable. At times, it short circuits the GOM and turns east towards the Florida Straits soon after entering the GOM. At other times, it extends all the way to the northeastern Gulf of Mexico continental shelf forming a large meander. Eddies pinch off the meandering Loop Current at irregular intervals, and form anti cyclonic warm core rings that propagate into the western GOM where they dissipate. Due to its limited size, the size of the state vector in high-resolution GOM-HYCOM configurations is  $O(10^6-10^7)$  and computationally expensive advanced assimilation schemes which require on the order of  $O(50-100)$  concurrent model runs can therefore be tested with high horizontal resolution GOM-HYCOM configurations. Furthermore, the GOM is well sampled by both remotely sensed and in-situ data.

In order to be able to test the ability of data assimilation schemes to perform in the presence of tides, we added tides to the “toolbox”. We used a  $1/25^\circ$  horizontal configuration with 20 layers. The eastern and southern boundaries are nested within the global  $1/12^\circ$  HYCOM. In order to avoid reflections due to the tides at the boundaries, a radiative *Flather* condition is applied on the barotropic components of the velocity. The initial condition corresponds to the condition of August 1<sup>st</sup> 2008 given by one of the assimilative simulation of the global  $1/12^\circ$  configuration of HYCOM (a strong loop current pattern is present, Figure 7). The atmospheric forcing is given by the Navy Operational Global Atmospheric Prediction System (NOGAPS). The barotropic tidal transport and elevation are prescribed at the open boundaries and are derived from the Egbert and Erofeeva (2002) model. We run the model for 30 days and all the analysis are done after day 8, time after which the model has reached an equilibrium state (the tidally averaged energy in the domain neither increases or decreases). Figure 7 shows the initial SSH for the full considered domain and highlight the presence of the loop current. We use the t-tide software to extract tidal harmonics. Figure 8 shows the tidal amplitudes (colored) and tidal phases (contoured) for: the main semidiurnal constituent ( $M_2$ , Figure 8a), the lunar diurnal tidal constituent ( $O_1$ , Figure 8b), and a comparison to the  $M_2$  computed from GOT99 (resolution is  $1/3^\circ$ ) (Figure 8c), and the  $O_1$  computed from GOT99 (Figure 8d). The location of the  $M_2$  amphidromic point (zero tidal elevation at any time) compares well with previous studies (Khanta, 2005; Gouillon et al., 2009) and the GOT99 (global ocean tide model from T/P altimetry; Ray, 1999) data and tidal amplitudes ( $\sim 30$  cm at the West Florida Shelf). The spatial homogeneity of the  $O_1$  tidal amplitudes and co-tidal lines also compares well to the GOT99 data and previous study. Figure 9 shows a snapshot of a cross-vertical section of meridional baroclinic velocity at  $89^\circ\text{W}$ . A typical internal wave vertical structure can be seen in the center of the basin where topography is rough and where bottom velocity can reach up to 15 cm/s. Strong internal tides that propagates throughout the domain are also generated at the West Florida Shelf (not shown here).

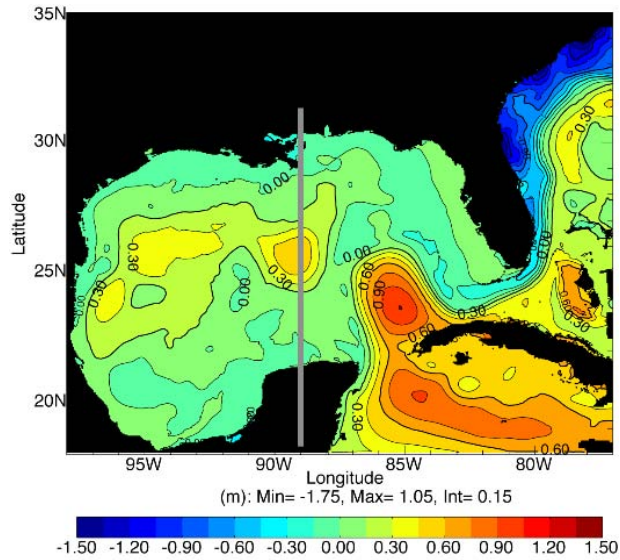


**Figure 7:** SSH (m) of the initial condition (August 2008) for the considered domain. The gray solid line shows the location of the cross-vertical section in Figure 9.

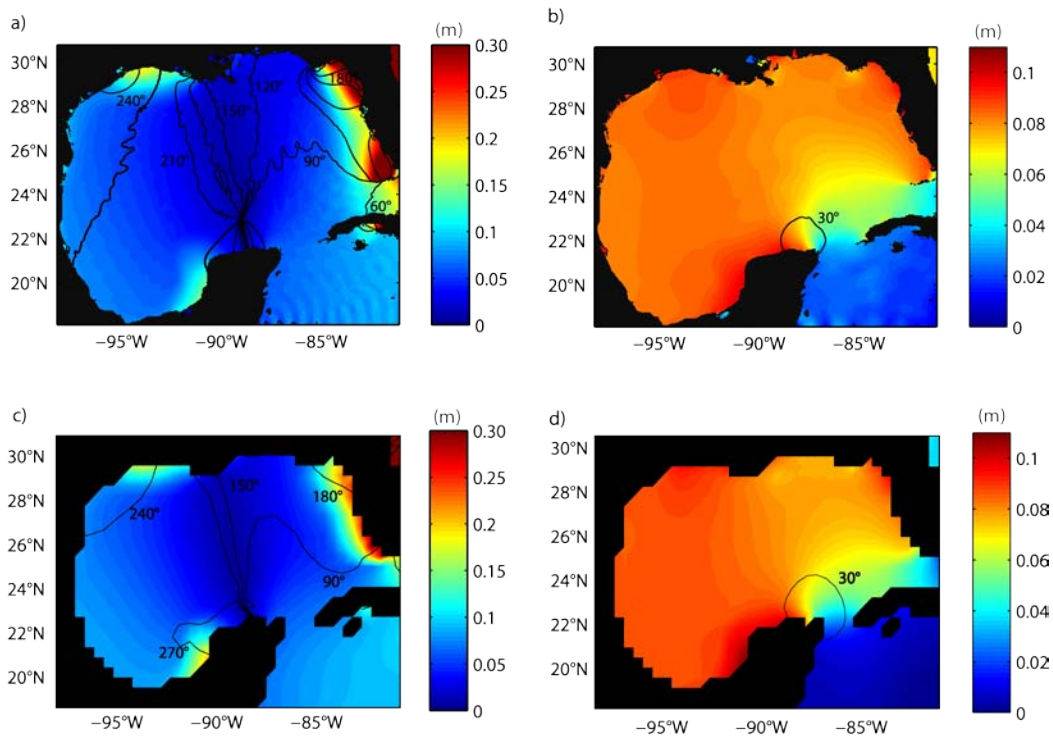


**Figure 8:** Maps of tidal amplitudes (colored) and phases (contoured) for: a) the M2 tidal constituent, b) the O1 tidal constituent, c) M2 from GOT99, and d) O1 from GOT99. Amplitudes are in meters and phases in degrees.

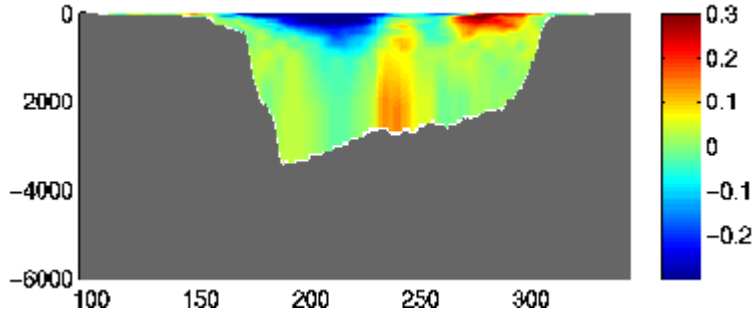


**Figure 9:** Snapshot of a cross-vertical section ( $89^{\circ}\text{W}$ ) of baroclinic meridional velocities. The abscissa is index of the model and ordinate is depth in meters.

### ARCTIC: Open ocean/ice interaction

The major goal of the work is to develop, validated, and improve a fully coupled modeling system of the Arctic Ocean and sea ice and to participate in the coordinated Arctic Ocean Model Intercomparison Project (AOMIP). The ocean model component is based on HYCOM. The sea ice component is based on CICE 4 (Hunke and Lipscomb, 2004). The model uses an Arctic dipole grid in two configurations:  $0.72^{\circ}$  (ARCc 0.72) and  $0.08^{\circ}$  (ARCc 0.08) horizontal resolution (courtesy of Wallcraft and Posey, NRL).

The initial configuration of the coarse resolution model (ARCc 0.72) had coastline that followed the 50 m isobath with closed Bering Strait (Figure 10) with an horizontal resolution in the Arctic Basin of about 30 km. The major purpose of this configuration was to perform several test runs to validate the ocean – sea ice coupling and the sensitivity of the numerical solution to forcing at the open boundaries (OBs). A model test simulation was run for 2003–2006 starting from PHC 3 climatology (<http://psc.apl.washington.edu/POLES>). At the lateral OBs, the model was relaxed to the climatological fields. At the surface, the model was forced with  $0.5^{\circ}$  3-hourly NOGAPS atmospheric fields.

The high resolution model (ARCc 0.08) has same domain configuration as ARCc 0.72, but the coastline is at the 10 m isobath and the Bering Strait is open. Horizontal resolution in the Arctic is 3 - 5 km. A test run was conducted for 2005-2008. The model was initialized from  $1/12^{\circ}$  global HYCOM and the lateral OBs used the fields from  $1/12^{\circ}$  global HYCOM. At the surface, the model was forced with  $0.5^{\circ}$  3-hourly NOGAPS atmospheric fields.

Both model runs have been validated against climatological fields. We find that:

- 1) The sea ice edge from simulated concentration fields matches satellite derived ice edge fairly well in the Arctic Ocean, but that the model tends to produce more ice in the Greenland Sea compared to observations.
- 2) The ocean surface temperature and salinity fields are in agreement with climatological fields (PHC 3 and GDEM 3) (Figure 11).
- 3) Both configurations fail to simulate the distribution and thermohaline characteristics of the Atlantic water (defined as water mass with  $T > 0^{\circ}\text{C}$ ) in the Arctic Ocean (Figure 12).

Possible reasons for misrepresentation of the Atlantic Layer in the simulations are as follows:

- (a) Insufficient vertical discretization in the deep ocean: Target densities are chosen such that the maximum vertical resolution is given to the ocean layer above the Atlantic water.
- (b) Atlantic water inflow to the Arctic Ocean is not correct.
- (c) Internal wave background diffusivity is to large.
- (d) In the ARCC 0.72: unresolved Siberian shelf and closed Bering Strait.

We are currently reconfiguring ARCC 0.72 using an improved bathymetry (Figure 1, right) and further analyzing ARCC 0.08.

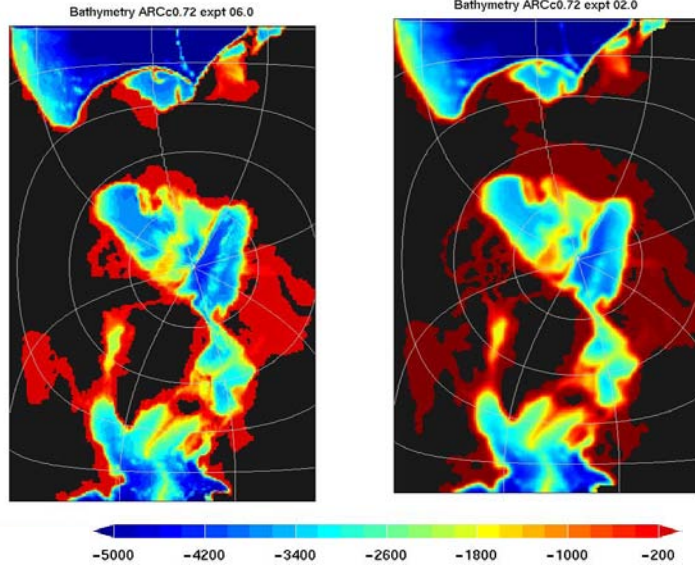


**Figure 10.** Model bathymetry of the ARCC 0.72. Land is dark grey. Left: existing model domain. Right: model domain with improved bathymetry: open Bering Strait, shallow coastline (10 m) resulting in a better representation of the Siberian shelf, better resolved channels in the Canada Arctic Archipelago.

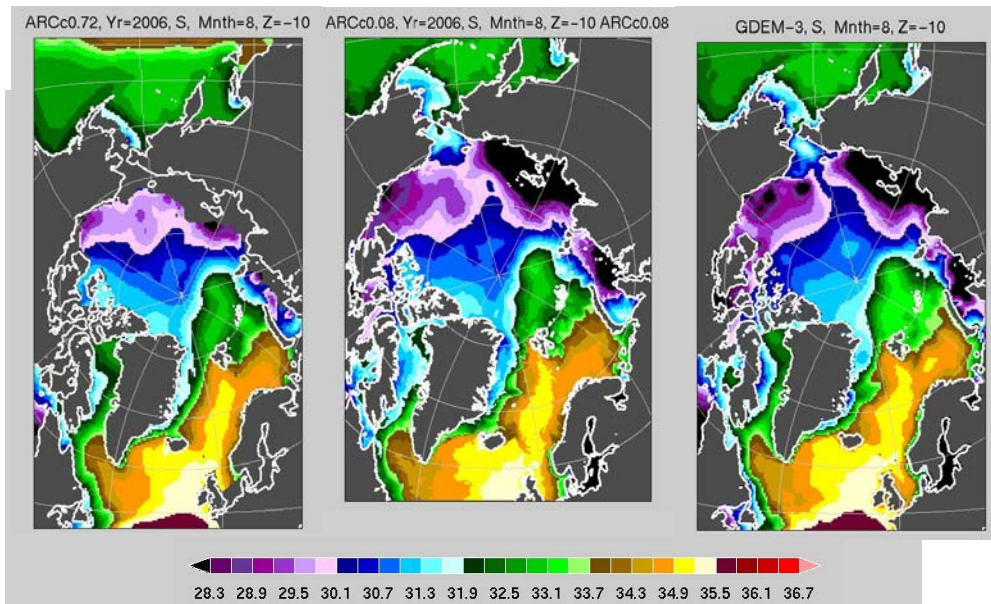


**Figure 11.** Salinity fields at 10 m. Left and Middle: from ARCC 0.72 and ARCC 0.08, respectively, in August 2006. Right: Climatological salinity field from GDEM 3.

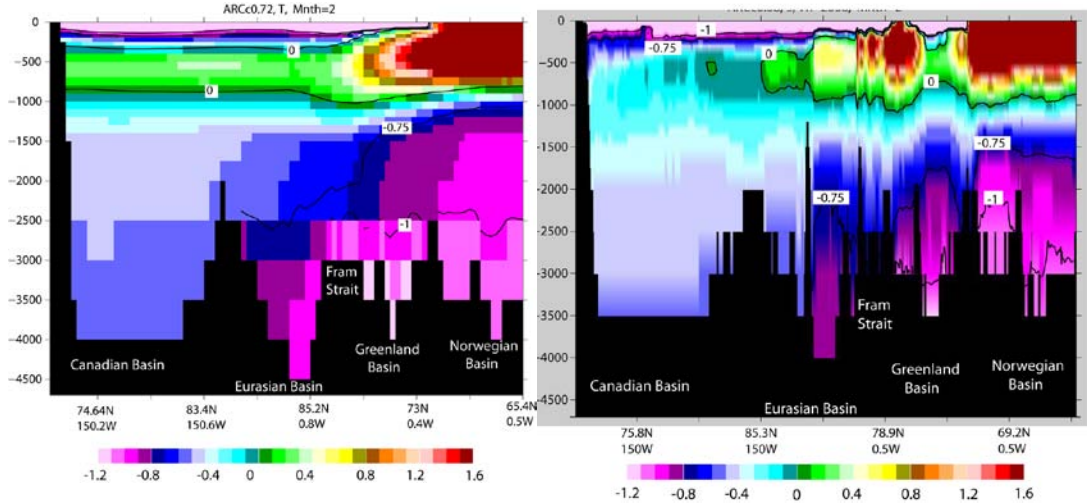


**Figure 12.** Vertical temperature distribution along the Arctic Ocean – Greenland Sea cross-section (along 150 W and 0W meridians). Left: from ARCC 0.72. Note the colder Atlantic Layer in the Eurasian Basin when compared to climatology. Right: from ARCC 0.08. The model has failed to simulate any Atlantic water in the Canadian Basin.

## IMPACT/APPLICATIONS

The  $1/25^\circ$  (3.5 km mid-latitude) resolution, first used in some FY09 global HYCOM simulations, is the highest so far for a global ocean model with high vertical resolution. A global ocean prediction system, based on  $1/25^\circ$  global HYCOM with tides, is planned for real-time operation starting in 2012. At this resolution, a global ocean prediction system can directly provide boundary conditions to nested relocatable models with  $\sim 1$  km resolution anywhere in the world, a goal for operational ocean prediction at NAVOCEANO. At present, regional and coastal models often include barotropic tidal forcing, but internal tides are not included in their open boundary conditions. By including tidal forcing and assimilation in a fully 3-D global ocean model, an internal tide capability will be provided everywhere and allow nested models to include internal tides at their open boundaries.

## TRANSITIONS

None.

## RELATED PROJECTS

The computational effort is supported by DoD HPC Challenge and non-challenge grants of computer time. In FY09,  $1/25^\circ$  and  $1/12^\circ$  global HYCOM ran under a new FY09-11 DoD HPC Challenge grant.

## REFERENCES

Bleck, R., 2002: An oceanic general circulation model framed in hybrid isopycnic-cartesian coordinates. *Ocean Modelling*, 4, 55-88.

Burchard, H., Rennau, H., 2008: Comparative quantification of physically and numerically induced mixing in ocean models. *Ocean Modeling*, 20, 293-311.

Chassignet, E.P., L.T. Smith, G.R. Halliwell, and R. Bleck, 2003: North Atlantic simulations with the HYbrid Coordinate Ocean Model (HYCOM): Impact of the vertical coordinate choice, reference density, and thermobaricity. *J. Phys. Oceanogr.*, 33, 2504-2526.

Chin-Bing, S.A., A. Warn-Varnas, D.B. King, K.G. Lamb, M. Teixeira, and J.A. Hawkins, 2003: Analysis of coupled oceanographic and acoustic soliton simulations in the Yellow Sea: a search for soliton-induced resonances. *Mathematics and Computers in Simulation*, 62, 11-20.

Cummings, J.A., 2005. Operational multivariate ocean data assimilation. *Quart. J. Royal Met. Soc.*, 131 (613), 3583-3604.

Di Lorenzo E., Young, W.R., and Llewellyn-Smith, S., 2006: Numerical and Analytical Estimates of the M2 Tidal Conversion at Steep Oceanic Ridges. *J. Phys. Oceanogr.*, 36, 1072-1084.

Egbert, G. D., Erofeeva, S. Y., 2002: Efficient Inverse Modeling of Barotropic Tides. *J. Atmosph and Oceanic Technology*, 19, 183-204.

Gouillon, F., Morey, S., Dukhovskoy, D., O'Brien, J. J., 2009: Forced tidal response in the Gulf of Mexico. Submitted to JGR-Ocean.

Griffies, S. M., Pacanowski, R. C., Hallber, R.W., 2000: Spurious diapycnal mixing associated with advection in a z-coordinate ocean model. *Mon. Weather Rev.* 128, 538-564.

Haidvogel, D. B., Beckman, A., 1999: Numerical Ocean Circulation Modelling of Series on Environmental Science and Management, vol. 2. Imperial College Press, London.

Halliwell, Jr., G.R., 2004: Evaluation of vertical coordinate and vertical mixing algorithms in the HYbrid-Coordinate Ocean Model (HYCOM). *Ocean Modelling*, 7, 285-322.

Hunke, E.C. and W.H. Lipscomb, 2004. CICE: the Los Alamos sea ice model documentation and software user's manual. <http://climate.lanl.gov/Models/CICE>

Kantha, L., 2005: Barotropic tides in the Gulf of Mexico. *Geophysical Monograph*, AGU, 161, 159-163.

Khatiwala, S., 2003: Generation of internal tides in an ocean of finite depth: Analytical and numerical calculations. *Deep-Sea Res. I*, 50, 3-21.

Legg, S., Huijts K. M. H., 2006: Preliminary simulations of internal waves and mixing generated by finite amplitude tidal flow over isolated topography *Deep-Sea Research II*, 53, 140-156.

Morales Maqueda, M. A., Holloway, G., 2006: Second-order moment advection scheme applied to Arctic Ocean Simulation. *Ocean Modelling*. 14, 197-221.

Ray R. D., A global ocean tide model from Topex/Poseidon altimetry: GOT99.2, NASA Technical Memo. 209478, Goddard Space Flight Center, Greenbelt, 58 pp., 1999.

Riemenschneider, U., Legg, S., 2007: Regional simulations of the Faroe Bank Channel overflow in a level model. *Ocean Modelling*. 17, 93-122

Srinivasan, A., Chassignet, E.P., Bertino, L., Brasseur, P., Chin, T.M., Counillon, F., Cummings, J., Smedstad, O.M., Thacker, W.C., Mariano, A.J., 2009. Comparison of sequential approaches data assimilation into HYCOM part I: Twin Experiments. To be submitted to Ocean Modeling.

## PUBLICATIONS (2008-2009)

Magaldi, M., T.M. Özgökmen, A. Griffa, E.P. Chassignet, M. Iskandarani, and H. Peters, 2008. Turbulent flow regimes behind a coastal cape in a stratified and rotating environment. *Ocean Modelling*, 25, pp. 65-82, doi:10.1016/j.ocemod.2008.06.006.

LaRow, T.E., Y.-K. Lim, D.W. Shin, E.P. Chassignet, and S. Cocke, 2008: High resolution ensemble Atlantic basin seasonal hurricane simulations. *J. Climate*, 21, 3191-3206.

Chassignet, E.P., and D.P. Marshall, 2008: Gulf Stream separation in numerical ocean models. In "Eddy-Resolving Ocean Modeling", M. Hecht and H. Hasumi, Eds., AGU Monograph Series, 39-62.

Hurlburt H.E., E.P. Chassignet, J.A. Cummings, A.B. Kara, E.J. Metzger, J.F. Shriver, O.M. Smedstad, A.J. Wallcraft, and C.N. Barron, 2008: Eddy-resolving global ocean prediction. In "*Eddy-Resolving Ocean Modeling*", M. Hecht and H. Hasumi, Eds., AGU Monograph Series, 353-382.

Kara, A.B., A.J. Wallcraft, P.J. Martin, and E.P. Chassignet, 2008: Performance of mixed layer models in simulating SST in the Equatorial Pacific Ocean. *J. Geophys. Res.*, **113**, C02020, doi:10.1029/2007JC004250.

Hurlburt, H.E., G.B. Brassington, Y. Drillet, M. Kamachi, M. Benkiran, R. Bourdalle-Badie, E.P. Chassignet, G.A. Jacobs, O. Le Galloudec, J.M. Lellouche, E.J. Metzger, O.M. Smedstad and A.J. Wallcraft, 2009. High-Resolution Global and Basin-Scale Ocean Analyses and Forecasts. *Oceanography*, 22, (3) 110-127.

Metzger, E.J., H.E. Hurlburt, A.J. Wallcraft, O.M. Smedstad, J.A. Cummings, and E.P. Chassignet, 2009. Predicting "Ocean Weather" using the 1/12 degree global HYbrid Coordinate Ocean Model (HYCOM). *HPCinsight*, Spring 2009, 46-48.

Goni, G., M. DeMaria, J. Knaff, C. Sampson, I. Ginis, F. Bringas, A. Mavume, C. Lauer, I.-I. Lin, P. Sandery, S. Ramos-Buarque, K. Kang, A. Mehra, E.P. Chassignet, and G. Halliwell, 2009. Applications of satellite-derived ocean measurements to tropical cyclone intensity forecasting. *Oceanography*, 22(3), 190-197.

Hernandez, F., L. Bertino, G.B. Brassington, E.P. Chassignet, J. Cummings, F. Davidson, M. Drevillon, G. Garric, M. Kamachi, J.-M. Lellouche, R. Mahdon, M.J. Martin, A. Ratsimandresy, and C. Regnier, 2009. Validation and intercomparison studies within GODAE. *Oceanography*, 22(3), 128-143.

Hurlburt, H.E., G.B. Brassington, Y. Drillet, M. Kamachi, M. Benkiran, R. Bourdalle-Badie, E.P. Chassignet, O. LeGalloudec, J.-M. Lellouche, E.J. Metzger, P.R. Oke, T. Pugh, A. Schiller, O.M. Smedstad, B. Tranchant, H. Tsujino, N. Usui, and A.J. Wallcraft, 2009. High resolution global and basin-scale ocean analyses and forecasts. *Oceanography*, 22(3), 110-127.

Dombrowsky, E., L. Bertino, G.B. Brassington, E.P. Chassignet, F. Davidson, H.E. Hurlburt, M. Kamachi, T. Lee, M.J. Martin, S. Mei, and M. Tonani, 2009. GODAE systems in operation. *Oceanography*, 22(3), 80-95.

Misra, V., S. Chan, R. Wu, and E.P. Chassignet, 2009. Air-sea interaction over the Atlantic warm pool in the NCEP CFS. *Geophys. Res. Lett.*, 36, L15702, doi:10.1029/2009GL038737.

Legg, S., Y. Chang, E.P. Chassignet, G. Danabasoglu, T. Ezer, A.L. Gordon, S. Griffes, R. Hallberg, L. Jackson, W. Large, T. Özgökmen, H. Peters, J. Price, U. Riemenschneider, W. Wu, X. Xu, J. Yang, 2009. Improving oceanic overflow representation in climate models: the Gravity Current Entrainment Climate Process Team. *Bull. Amer. Met. Soc.*, 90(4), 657-670, doi: 10.1175/2008BAMS2667.1.

Cornillon, P., J. Adams, M.B. Blumenthal, E.P. Chassignet, E. Davis, S. Hankin, J. Kinter, R. Mendelsohm, J.T. Potemra, A. Srinivasan, and J. Sirott, 2009. NVODS and the development of OPeNDAP - an integrative tool for oceanographic data systems. *Oceanography*, 22(2), 116-127.

Chassignet, E.P., H.E. Hurlburt, E.J. Metzger, O.M. Smedstad, J. Cummings, G.R. Halliwell, R. Bleck, R. Baraille, A.J. Wallcraft, C. Lozano, H.L. Tolman, A. Srinivasan, S. Hankin, P. Cornillon, R. Weisberg, A. Barth, R. He, F. Werner, and J. Wilkin, 2009. U.S. GODAE: Global Ocean Prediction with the HYbrid Coordinate Ocean Model (HYCOM). *Oceanography*, 22(2), 64-75.

Rousset, C., M.-N. Houssais, and E.P. Chassignet, 2009. A multi-model study of the restratification phase in an idealized convection basin. *Ocean Modelling*, 26, 115-133, doi:10.1016/j.ocemod.2008.08.005.

Griffies, S.M., A. Biastoch, C. Boening, F. Bryan, G. Danabasoglu, E.P. Chassignet, M.H. England, R. Gerdes, H. Haak, R.W. Hallberg, W. Hazeleger, J. Jungclaus, W.G. Large, G. Madec, A. Pirani, B.L. Samuels, M. Scheinert, A.S. Gupta, C.A. Severijns, H.L. Simmons, A.-M. Treguier, M. Winton, S. Yeager, and J. Yin, 2009. Coordinated Ocean-Ice Reference Experiments (COREs). *Ocean Modelling*, 26, 1-46, doi:10.1016/j.ocemod.2008.08.007.